2004 Workshop on the Nuclear Radiology
of Breast Cancer
Rome (Italy) October 22-23, 2004

«Physica Medica» · Vol. XXI, Supplement 1, 2006

# Impact of High Energy Resolution Detectors on the Performance of a PET System Dedicated to Breast Cancer Imaging

Craig S. Levin, Angela M. K. Foudray, Frezghi Habte

*Department of Radiology and Molecular Imaging Program Stanford University School of Medicine, Stanford (USA)*

## *Abstract*

We are developing a high resolution, high sensitivity PET camera dedicated to breast cancer imaging. We are studying two novel detector technologies for this imaging system: a scintillation detector comprising layers of small lutetium oxyorthosilicate (LSO) crystals coupled to new position sensitive avalanche photodiodes (PSAPDs), and a pure semiconductor detector comprising cadmium zinc telluride (CZT) crystal slabs with thin anode and cathode strips deposited in orthogonal directions on either side of each slab. Both detectors achieve 1 mm spatial resolution with 3-5 mm directly measured photon interaction depth resolution, which promotes uniform reconstructed spatial resolution throughout a compact, breast-size field of view. Both detector types also achieve outstanding energy resolution (< 3% and < 12%, respectively for LSO-PSAPD and CZT at 511 keV). This paper studies the effects that this excellent energy resolution has on the expected system performance. Results indicate the importance that high energy resolution and narrow energy window settings have in reducing background random as well as scatter coincidences without compromising statistical quality of the dedicated breast PET data. Simulations predict that using either detector type the excellent performance and novel arrangement of these detectors proposed for the system facilitate ~20% instrument sensitivity at the system center and a peak noise-equivalent count rate of > 4 kcps for 200 microCi in a simulated breast phantom.

KEYWORDS: Breast cancer imaging, PET, detectors, cadmium zinc telluride, scintillation detectors, position sensitive avalanche photodiodes.

## 1. Introduction

Positron Emission Tomography (PET) is a non-invasive, *in-vivo*, functional and molecular imaging technology that has shown promise for more specific identification of cancer due to its unique ability to sense and visualize increased biochemical and molecular changes in malignant compared to healthy tissue. However, to date conventional PET has not been incorporated into standard practice for breast cancer management due to: [1] awkward, low photon efficiency geometry for breast imaging and relatively long scan times/low throughput of standard PET systems, [2] non-optimal spatial and contrast resolutions for early breast cancer identification, [3] relatively high cost; and [4] the lack of tracers with adequate specificity.

Low coincident photon detection efficiency (~ 1%) of the conventional clinical PET system limits the statistical quality of the data and achievable reconstructed spatial resolution, which reduces detection sensitivity for small lesions. Low efficiency also means relatively long scan times, which, together with the inappropriate large diameter ring geometry, make conventional PET impractical for breast imaging. Low detection efficiency together with inadequate spatial resolution (6-12 mm) mean poor visualization of lesions smaller than 0.5 $cm^3$, which further reduces PET's sensitivity for early detection of breast cancer, associated metastases, or monitoring after therapeutic interventions or treatments. Improved delineation of smaller lesions is important since it translates to earlier detection and improved prognosis of malignant tumors and their metastases [1]. The open geometry and relatively poor energy and coincident time resolutions of conventional PET systems increases acceptance of background scatter and random photon coincidence events from both within and outside the camera field-of-view (FOV), which reduces achievable contrast resolution. Finally, the relatively high cost for standard PET instrumentation limits PET's cost-effectiveness for a variety of breast cancer indications.

We are developing a PET system dedicated to breast cancer imaging that will address the issues of low photon detection efficiency, long scan times, awkward geometry, non-optimal spatial and energy resolutions, and high cost of PET for breast cancer imaging. Just as a dedicated system (mammography) is required to optimize X-ray breast imaging, we argue that a dedicated camera is crucial to optimize PET breast imaging, and without such a system, we are far from reaching PET's potential to play a role in breast cancer management. A new high performance detector will be configured into a compact system dedicated to close-proximity, breast and/or axillary node imaging with very high coincident photon detection efficiency and ultra-high spatial, energy, and coincident time resolutions. If used in conjunction with a highly specific breast cancer tracer, this high photon efficiency and high spatial resolution imaging system would facilitate the early

Address for correspondence: Craig S. Levin, Ph.D., Stanford University School of Medicine, 300 Pasteur Drive, MC 5128 Alway Building, Room M001 Stanford, CA 94305-5128, Phone: 650-736-7211, Fax: 650-724-1499. E-mail: cslevin@stanford.edu

identification of developing, spreading or recurring breast cancer. Using a tracer with non-specific uptake (e.g. Fluorodeoxyglucose (FDG)], there will likely be activity generated from the nearby heart and liver. Excellent energy and time resolutions and flexible positioning of the camera to reduce out of FOV activity will help to reduce the resulting high background scatter and random coincidence rates that can degrade lesion contrast resolution. As is true for mammography, imaging the chest wall at close proximity is challenging. However, a dedicated breast imaging geometry may be opened wider and oriented favorably to contain the chest wall. Finally, a small, relatively inexpensive camera dedicated to breast imaging could significantly reduce study costs of the technique to the point that it becomes cost-effective for a variety of breast cancer indications.

The 511 keV photon detectors used and their geometrical configuration about the patient determine the resulting performance characteristics of the dedicated breast imaging system. The system performance goals are 1 $mm^3$ spatial resolution achieved uniformly within the FOV, > 10% coincidence detection efficiency (a.k.a. *photon sensitivity*), and ≥12% energy resolution for 511 keV photons. In this paper we discuss the importance of using 511 keV detectors with very high energy resolution configured into a high photon sensitivity system for dedicated PET imaging of the breast. We demonstrate that for a PET system built with detectors that have excellent energy resolution, one may use a very narrow energy window setting to significantly reduce both scatter and random coincidence events to obtain high contrast resolution, while also achieving high counting statistics and signal-to-noise ratio (SNR) within that narrow window.

## 2. Materials and Methods

### 2.1. *511 keV photon detectors under study*

In this paper we studied two types of high performance 511 keV photon detector modules that are candidates for the breast imaging system. The first detector module design uses 1 mm lutetium oxyorthosilicate (LSO) scintillation crystal pixels coupled to new position sensitive avalanche photodiodes (PSAPD) [2, 3]. The crystals are coupled to the PSAPD in a novel configuration that promotes nearly complete (> 90%) scintillation light collection efficiency independent of photon interaction depth [2]. Incoming photons see ≥ 2 cm thick LSO for high (> 82%) intrinsic (single 511 keV photon) detection efficiency. The PSAPD and crystal segmentation facilitate direct measurement of photon interaction depth within the scintillation crystal array [2, 3] (Figure 1, *left*). The other detector under study is cadmium zinc telluride (CZT) semiconductor crystal with a cross-strip cathode (top surface) and anode (bottom surface) electrode patterns. These CZT arrays are arranged in an innovative 'edge-

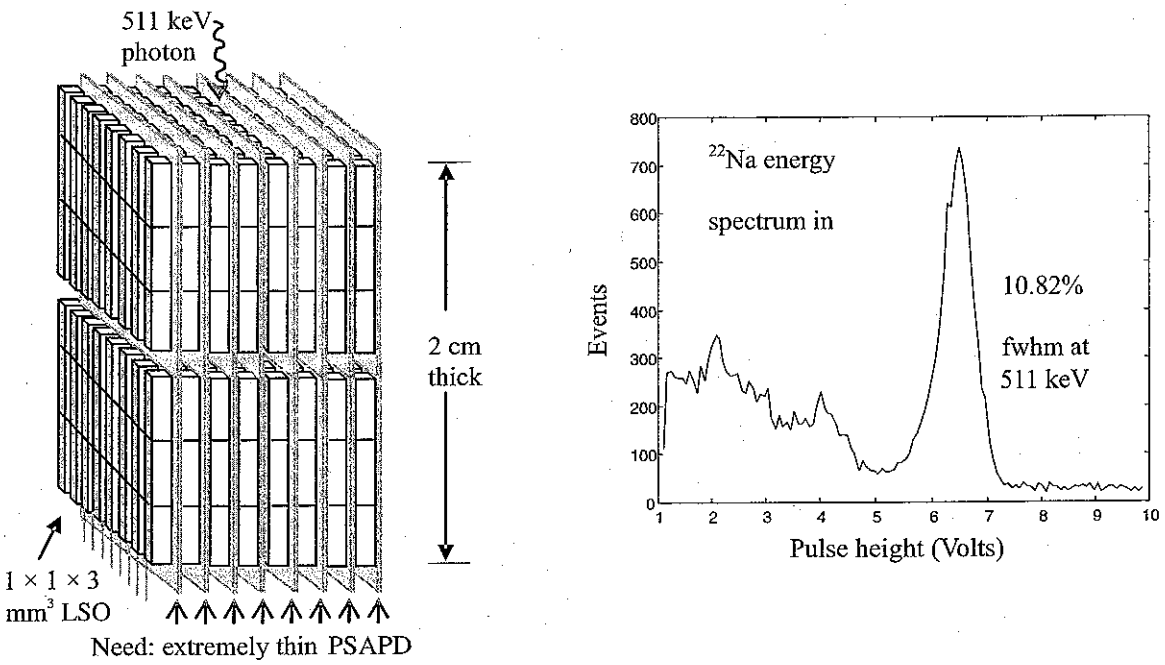


Fig. 1. *Left*: Depiction of proposed position sensitive 511 keV photon scintillation detector module. The detector comprises layers of 1 mm LSO crystal arrays (white) coupled to PSAPDS (gray) in a novel sideways arrangement that promotes uniform and high light collection efficiency. Each layer has two separate crystal arrays coupled to separate PSAPD chips. Incoming photons see a minimum thickness of ~2 cm of LSO with directly measured interaction depth resolution of 3 mm. Extremely thin PSAPDS are required to preserve a high crystal packing fraction. *Right*: $^{22}Na$ energy spectrum extracted from one 1 × 1 × 3 mm LSO crystal from one LSO-PSAPD array layer.

on' orientation (Figure 2, *left*) that allows incoming photons to see > 4 cm thick CZT for high (> 86%) intrinsic 511 keV photon detection efficiency [4]. These detectors also have three-dimensional (3-D) photon interaction positioning capabilities within the detector volume [4]. Figures 1 and 2 (right) also show 511 keV photon energy spectra acquired in the two novel detectors demonstrating the excellent energy resolution performance of < 3 and < 12% full-width-at-half-maximum (fwhm) energy resolution achieved, respectively, for the CZT and LSO-PSAPD detectors. The measured coincidence time resolution spectra measured for the two detector types had typical values of 2 and 8 ns fwhm, respectively for the LSO-PSAPD, and CZT detectors. The time resolution of the CZT is relatively poor compared to LSO since semiconductor detectors rely on charge transport rather than scintillation light transport for their signal formation.

### 2.2. *Monte Carlo Simulations of Detector Gantry*

We used Monte Carlo simulations [5] to study the geometrical configuration and performance of a dedicated breast imaging PET system built from the proposed position sensitive photon detector arrays. We studied dual-plate [6] as well as 'box' [7] configurations of the detector modules (Figure 3). In this paper we focus on results of photon sensitivity and SNR of PET data for the box configuration using Monte Carlo simulated PET acquisitions that incorporated the accurate geometry, including all expected dead gaps, of the PET detector modules arranged in the box arrangement. The inner box gantry FOV dimensions for both types of detector systems (CZT or LSO-PSAPD) were $16 \times 16 \times 12$ cm$^3$. The box thickness is 2 cm using the LSO-PSAPD or 4 cm using CZT (Figures 1 and 2). For all simulations we assumed the experimentally meas-

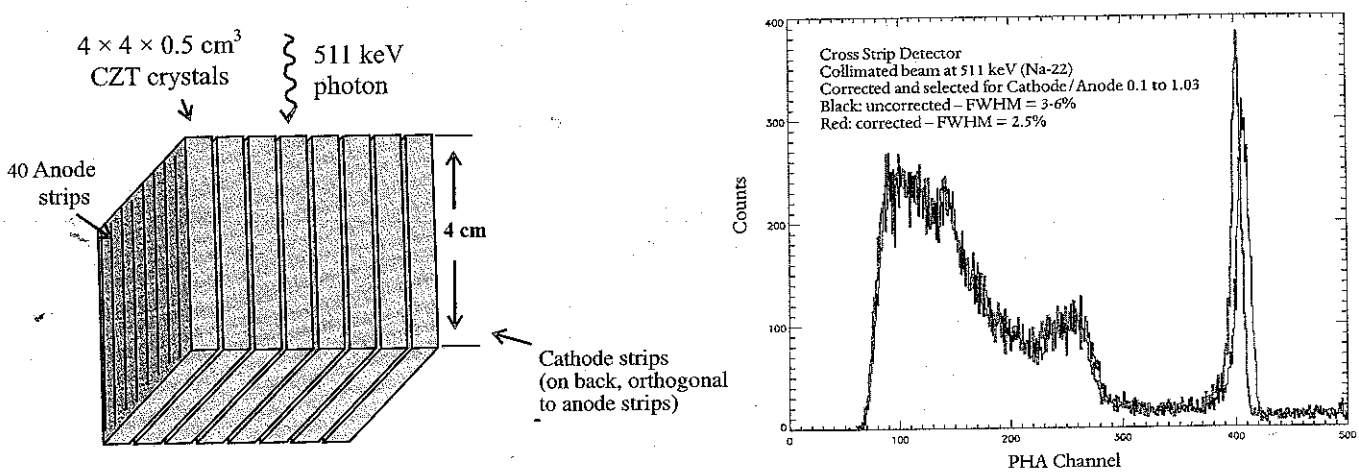


FIG. 2. *Left*: Depiction of proposed position sensitive 511 keV photon semiconductor detector module. The detector comprises layers of 40 × 40 × 5 mm$^3$ CZT (grey). Orthogonal strips of cathodes and anode electrodes are deposited on each side of each CZT slab. Signals induced on the anodes, cathodes, as well as their ratio are used to determine the 3-D interaction coordinates. The detector arrays are arranged edge-on so that incoming 511 keV photons see a minimum thickness of ~4 cm of CZT with directly measured interaction depth resolution of 3-5 mm. The CZT layers can be packed together with > 99% packing fraction. *Right*: $^{22}$Na energy spectrum extracted from one CZT slab layer before (black) and after (grey) correction for variations in charge collection for different interaction locations between the anode and cathode using the ratio of cathode/anode signals.

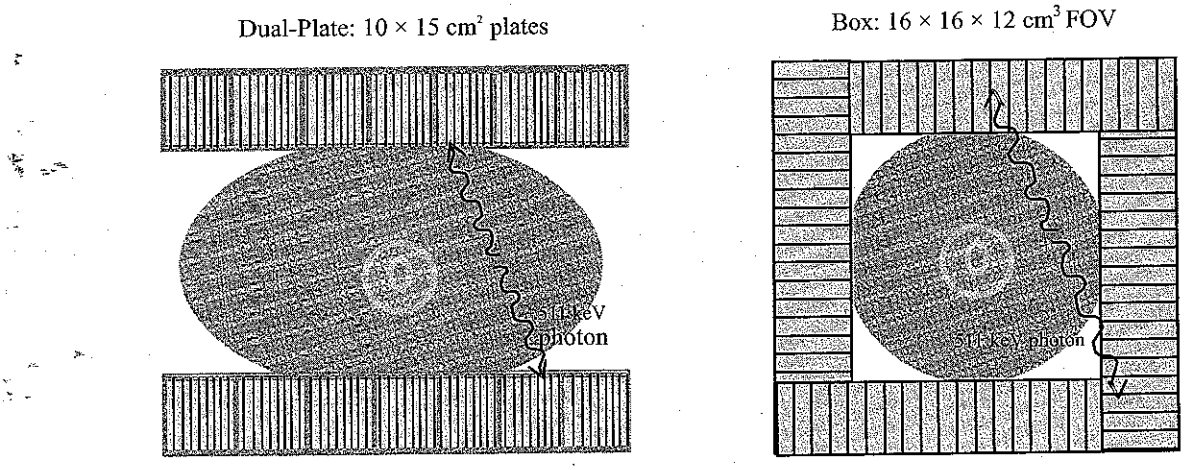


FIG. 3. Two potential configurations of the proposed LSO-PSAPD or CZT detector modules. *Left*: Dual-plate configuration; *Right*: Box configuration. This paper focuses on performance results of the box configuration.

ured values of 3 and 12% fwhm energy resolution at 511 keV, and 8 and 2 ns fwhm coincidence time resolution, respectively for the LSO-PSAPD and CZT detector configurations. For the photon sensitivity studies, we translated (in simulations) a point source of annihilation photons from the center to the edge of the FOV of the box along the center 'axis' of the box and measured the total number of coincident 511 keV photon pairs detected within the detectors for various energy and coincidence time window settings. For the measure of SNR of the dedicated breast PET system data, the $16 \times 16 \times 12$ $cm^3$ sensitive volume of the system was completely filled with water-equivalent breast tissue containing a uniform distribution of 200 μCi (7.4 Mbq) of $^{18}F$ activity, which is consistent with expected $^{18}F$ FDG uptake in breast tissue. The figure of merit used for the SNR of acquired data was noise-equivalent counts (NEC) defined as $T^2/(T+S+2R)$, where T is the true coincident event rate and S (R) are the undesirable background scatter (random) coincidence event rates for a given configuration. For NEC calculations, completely filling the active volume of the system with activity represents the worse case scenario, however out of FOV activity such as from the hot heart or liver that could have important impact on detected event rates in a dedicated breast geometry was not simulated in this study.

## 3. Results

Figure 4 plots coincident photon detection efficiency (photon sensitivity) as function of position along the axis from the center to the edge for both the LSO-PSAPD and CZT systems for two different energy windows ($2\times$ and $3\times$ the energy resolutions) and coincident time windows equal to $2\times$ and $1\times$ the coincidence time resolutions, respectively for the LSO-PSAPD and CZT detector types. Near the system center the predicted point source photon sensitivity is ~20% for both detector types. Figures 5-8 plot the true, scatter, random and NEC coincidence rate as a function of energy window for different time windows and as a function of coin-

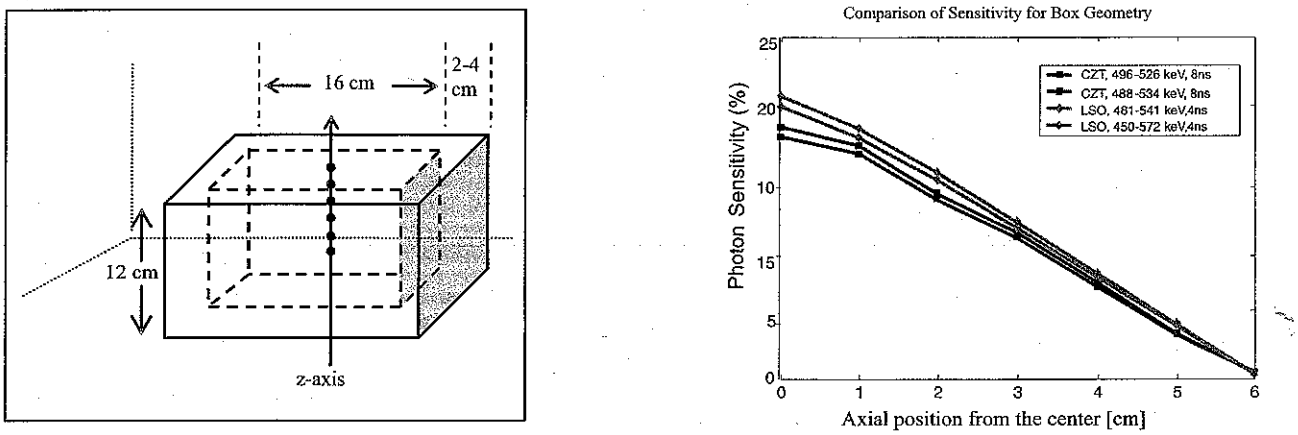


Fig. 4. *Left*: A point $^{18}F$ source was translated from the center to the FOV edge along the axis of a box configuration of detectors. *Right*: Photon sensitivity (coincident photon detection efficiency) vs axial position using the proposed CZT and LSO-PSAPD position sensitive detectors systems for the narrow energy window settings shown.

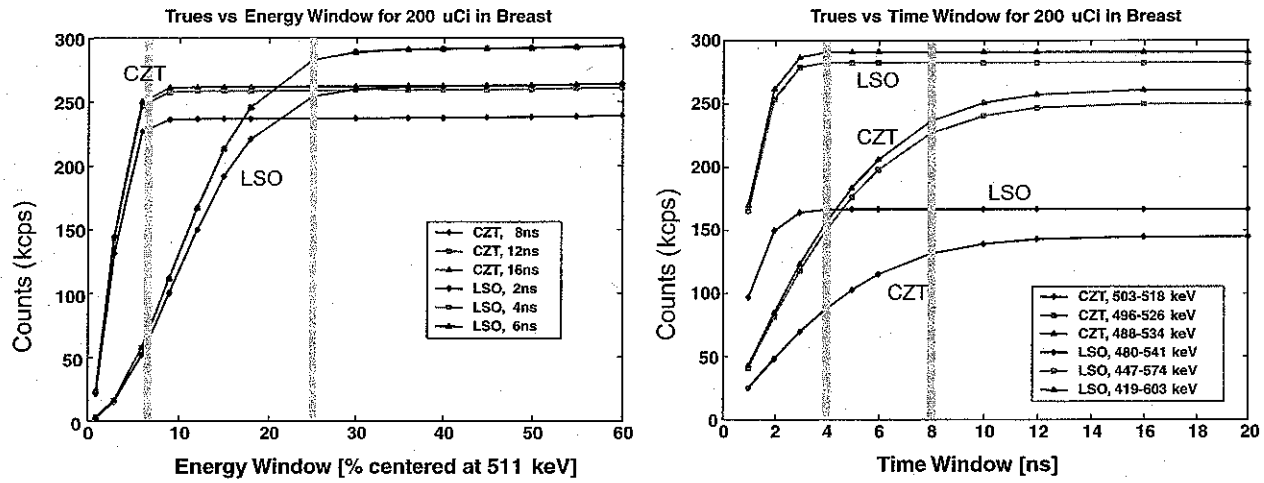


Fig. 5. True coincidence rate for CZT and LSO-PSAPD detector systems vs energy window setting for various coincidence time windows (*left*) and vs coincidence time window for various energy windows (*right*). For the simulations, 200 μCi of activity was uniformly distributed in simulated breast tissue that completely filled the $16 \times 16 \times 12$ $cm^3$ box volume.

cidence time window for different energy windows for the two detector systems. The peak NEC values are 4.2 and 4.3 kcps using 24 and 6% energy window and 4 and 8 ns time window, respectively, for LSO-PSAPD and CZT detectors and 200 μCi total activity uniformly distributed within the 16 × 16 × 12 $cm^3$ simulated breast tissue volume.

## 4. Discussion

Figure 4 shows that unprecedented photon sensitivity (20%) near the center is possible with a dedicated breast PET geometry that collects photons at close proximity, using relatively thick, tightly packed detector crystals for either the LSO-PSAPD or CZT detectors that are proposed. As with any 3-D PET system, the sensitivity drops off rapidly as the point source approaches the edge of the sensitive FOV.

Figure 5 shows that relative to the CZT design, the LSO-PSAPD box configuration has a 10-15% higher true coincident rate for an energy window equal to twice the energy resolution for each detector type and a time window equal to 4 ns for the LSO-PSAPD design and 8 ns for the CZT system. This higher trues rate is likely due to the fact that LSO has a higher probability for photoelectric absorption and the coincidence time window setting for the simulated LSO-PSAPD system was 2× the time resolution rather than 1 × the time resolution for the simulated CZT design. However, as seen in Figure 6, the scatter coincidence rate is nearly a factor of eight lower for the CZT compared to the LSO-PSAPD system, since the 511 keV photopeak energy resolution and window setting is significantly narrower (3% fwhm and 6%, respectively for CZT and 12% fwhm and 24%, respectively for LSO-PSAPD).

Figure 7 shows that due to the superior coincidence time resolution for the LSO-PSAPD (2 ns fwhm) compared to the CZT (8 ns fwhm) configuration, the random coincidence rate is generally lower. *However*, for the proposed CZT coincidence time window of 8 ns and energy window of 6% (496-526 keV), the random coincidence rate is comparable for both the CZT (~9 kcps) and LSO-PSAPD (~11 kcps) designs. The reason for this is that that the random coincidence rate varies as the square of the singles rate, but only to the first power of the coincidence time window. The singles rate varies with the energy window width. Thus, the random coincidence rate varies as the square of the energy window and using a narrow energy window will reduce the random coincidence rate significantly. This is a result of the fact that many detected single photons undergo scatter in the tissue before absorption in the detector material and a narrow energy window helps to reject such events. Thus, even though the coincidence time resolution is relatively poor for CZT, the excellent energy resolution and narrow energy window setting keep the random coincidence rate under control.

Figure 8 shows that both the LSO-PSAPD and CZT box configurations have similar peak NEC values, assuming a total of 200 μCi uptake in the breast tissue. The LSO-PSAPD achieves this peak at lower coincidence time window setting of 4 ns compared to 8 ns for the CZT design, but at a higher energy window of 24% compared to 6% for the CZT. The CZT's excellent energy resolution (3% fwhm) and narrow window (6%) allows superior rejection of scatter coincidences and makes up for the relatively poor coincidence time resolution (8 ns fwhm) to control random coincidence rate. Thus, the CZT system achieves similar peak NEC performance to the LSO-PSAPD system. Similar effects of reduced randoms rate with higher energy resolution and narrow energy window setting were seen with a mouse and rat phantom in a dedicated CZT small

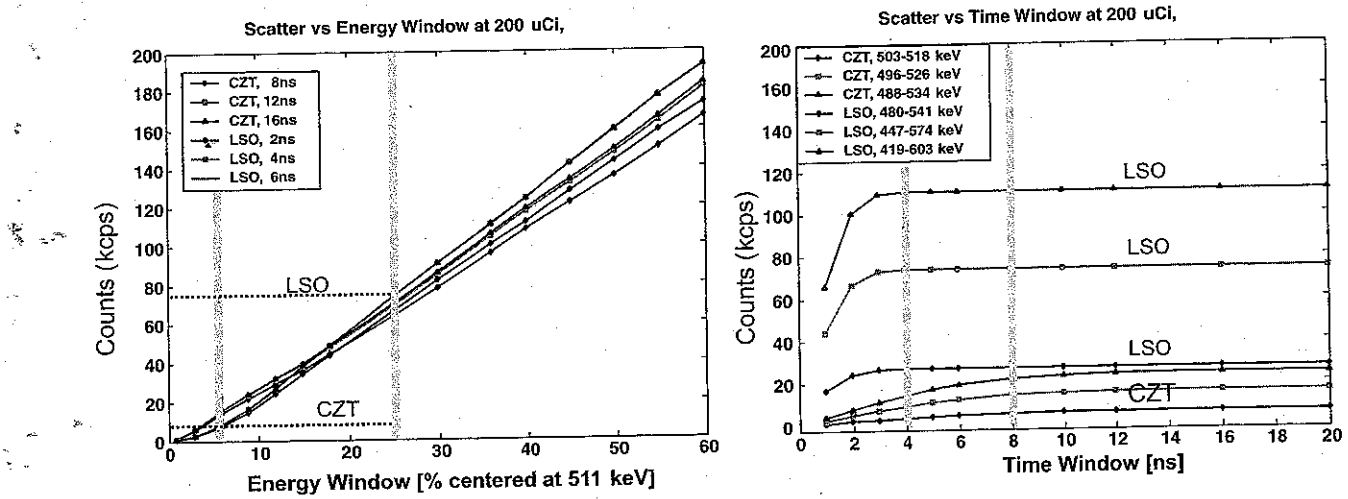


Fig. 6. Scatter coincidence rate for CZT and LSO-PSAPD detector systems vs energy window setting for various coincidence time windows (*left*) and vs coincidence time window for various energy windows (*right*). For the simulations, 200 μCi of activity was uniformly distributed in simulated breast tissue that completely filled the 16 × 6 × 12 $cm^3$ box volume.

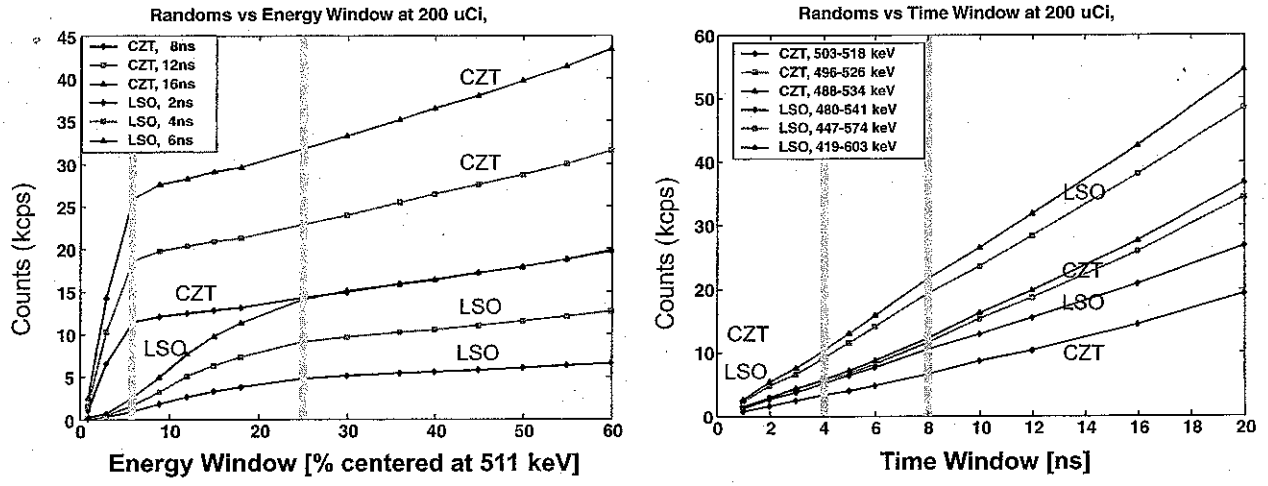


Fig. 7. Random coincidence rate for CZT and LSO-PSAPD detector systems vs energy window setting for various coincidence time windows (*left*) and vs coincidence time window for various energy windows (*right*). For the simulations, 200 μCi of activity was uniformly distributed in simulated breast tissue that completely filled the 16 × 16 × 12 cm³ box volume.

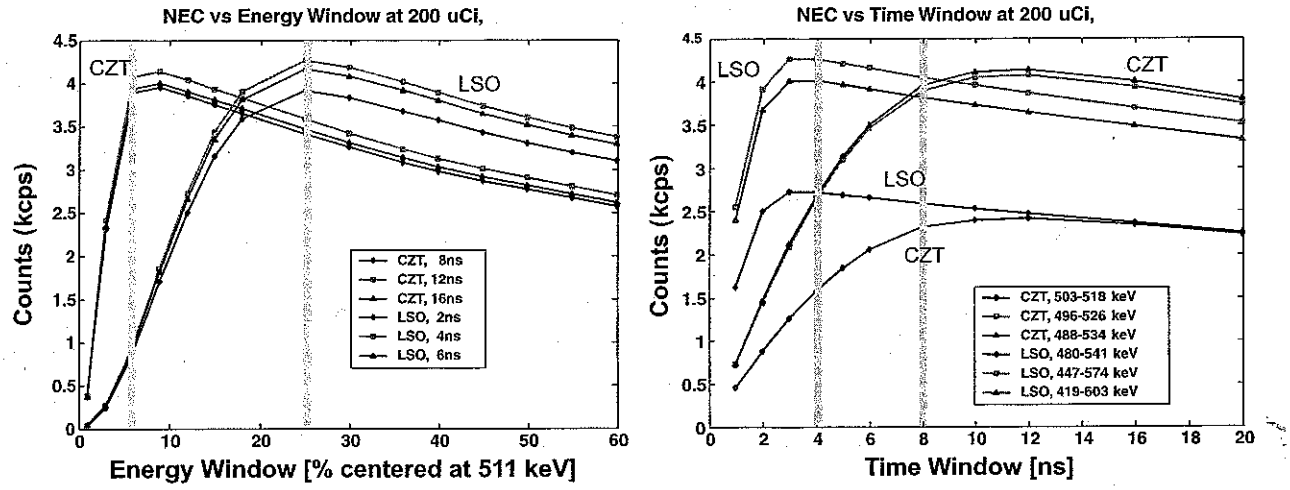


Fig. 8. Noise-equivalent count rate (NEC) for CZT and LSO-PSAPD detector systems vs energy window setting for various coincidence time windows (*left*) and vs coincidence time window for various energy windows (*right*). For the simulations, 200 μCi of activity was uniformly distributed in simulated breast tissue that completely filled the 16 × 16 × 12 cm³ box volume.

animal PET system [4]. More realistic simulated breast phantom configurations should also include out of FOV activities from organs such as the heart or liver, which this study did not address. However, with a more realistic phantom we expect the same general trends we have observed here to hold for both detector systems under study.

## 5. Conclusion

Results from simulation of a dedicated PET breast imaging geometry indicate that using detectors with excellent (< 12% fwhm) 511 keV energy resolution, one may use a very narrow energy window setting to reject random in addition to scatter coincidences for high contrast resolution, while maintaining high true coincidence counts and SNR. This important effect of energy resolution makes the use of CZT feasible in PET even though its coincidence time resolution is poor. The detector configuration proposed yields nearly 20% instrument sensitivity that facilitates the reconstructed spatial resolution goal of 1 mm³ with high SNR. These qualities of outstanding spatial resolution and contrast resolution translate into superior lesion visualization and quantitative accuracy.

## Acknowledgements

The authors would like to thank Dr. James Matteson at the UC San Diego Center for Astrophysics and Space Studies (CASS) for his help with developing and testing CZT detectors and Richard Farrell from RMD, Inc. for his efforts to develop an extremely thin PSAPD device. This work was supported in part by NIH-NCI grants R21 CA098691 and RO1CA119056 and UC Breast Cancer Research Program grant 12IB-0092.

## References


[1] Silverstein M J, Lagios M D, Groshen S, Waisman J R, Lewinsky B S, Martino S, Gamagami P, Colburn W J. The influence of margin width on local control of ductal carcinoma in situ of the breast. N Engl J Med 1999: 340; 1455-1461.

[2] Levin C S. Design of a high-resolution and high-sensitivity scintillation crystal array for PET with nearly complete light collection. IEEE Transactions On Nuclear Science Part 1 Oct 2002: 49 (5); 2236-2243.

[3] Levin C S, Foudray A M K, Olcott P D *et alii*. Investigation of position sensitive avalanche photodiodes for a new high-resolution PET detector design. IEEE Transactions On Nuclear Science Part 2 Jun 2004 51 (3); 805-810.

[4] Levin C S, Matteson J, Habte F, Skelton T, Pelling M, Duttweiler F. Promising Characteristics and Performance of Cadmium Zinc Telluride Detectors for Positron Emission Tomography. Presented at the 2004 IEEE Nuclear Science Symposium and Medical Imaging Conference, Rome (Italy), October 2004. Abstract # M2-117, Book of Abstracts, P. 136, IEEE Nuclear and Plasma Sciences Society.

[5] Strul D, Santin G, Lazaro D, Breton V, Morel C. gate (GEANT4 Application for Tomographic Emission): a PET/SPECT general-purpose simulation platform. Nucl Phys B (Proc Suppl) 2003; 75-79.

[6] Weinberg I N, Beylin D, Zavarzin V *et alii*. Positron emission mammography: High resolution biochemical breast imaging. Technology in Cancer Research and Treatment 2005 Feb: 4 (1).

[7] Moses W W, Qi J Y. Instrumentation Optimization For Positron Emission Mammography Nuclear Instruments & Methods. In: Physics Research Section A, Accelerators Spectrometers Detectors And Associated Equipment Jul 11 2004: 527 (1-2); 76-82.